



Poisson Noise Removal From Fluorescence Images Using Optimized Variance-Stabilizing Transformations And Standard Gaussian Denoising Strategies.

* K.Sampath Kumar ** C. Arun

* Assistant Professor, Sri Venkateswara College Of Engineering & technology, Chennai

** Associate Professor, R. M. K. College of Engineering & technology, Chennai

ABSTRACT

We propose a methodology of noise removal mainly intended for fluorescence images. The main component of noise in fluorescence images is Poisson noise. First, we Gaussianize the image, i.e., the noise variance is stabilized by applying the Anscombe root transformation to the data, producing a signal in which the noise can be treated as additive Gaussian with unitary variance. The resulting image is then denoised using a conventional denoising algorithm for additive white Gaussian noise. Third, an inverse transformation is applied to the denoised signal, obtaining the estimate of the signal of interest. The choice of the proper inverse transformation is crucial for fluorescence images in order to minimize the bias error which arises when the nonlinear forward transformation is applied. We study the impact of optimal inverse transform for the Anscombe transformation suitable for fluorescence images, in particular the exact unbiased inverse. We show that the estimation can be consistently improved by applying the exact unbiased inverse, particularly at the low-count regime. This results in a very competent filtering solution that is competitive with some of the best existing methods for Poisson image denoising.

Keywords : Fluorescence images, Poisson noise and Anscombe transformation.

Introduction

In this paper we aim at finding out best methods for denoising images acquired through fluorescence microscopy. With the recent development of fluorescent probes and new high-resolution microscopes, biological imaging has entered a new era and is presently having a profound impact on the way research is being conducted in the life sciences. Biologists have come to depend more and more on imaging. They can now visualize sub cellular components and processes in vivo, both structurally and functionally. Observations can be made in two or three dimensions, at different wavelengths (spectroscopy), possibly with time-lapse imaging to investigate cellular dynamics. In fluorescence microscopy, only a few photons are collected by the photo sensors, due to various physical constraints (low-power light source, short exposure time, photo toxicity). Under these imaging conditions, the signal-to-noise ratio (SNR) of such images is signal dependent and varies across the image plane. The number of photons actually hitting the sensor during a given time interval (exposure time) may not be exactly the expected value. These values are distributed around the expected value according to a Poisson distribution. The difference is seen especially with short exposure times or low light conditions (the lesser photons there are, the more the fluctuations relatively affect). Thus for such Poisson images the general goal of denoising is to approximate the expected value, and thus remove the random noise. Usually we have only one image, contaminated by one realization of the random noise, which makes it harder to approximate the underlying

true value. Most denoising algorithms make the simplifying assumption that the noise is Gaussian.

It is established the additive Gaussian noise model is a poor description of the actual photon-limited image recording, compared with that of a Poisson process. This motivates the use of restoration methods optimized for Poisson noise distorted images.

As the noise variance in Poisson noise equals the expected value of the underlying true signal, Poisson noise is signal dependent, which makes the premise for Poisson denoising very different from the case of additive white Gaussian noise with constant variance typically assumed by signal processing filters.

Although denoising algorithms specifically designed for Poisson noise have been proposed (e.g., [1], [2], [3], [4], [5]), often the removal of Poisson noise is performed through the following three-step procedure. In this paper we apply this three step procedure and study in detail denoising in fluorescent images which are affected by Poisson noise.

First, the noise variance is stabilized by applying the Anscombe root transformation

$$: \rightarrow 2\sqrt{I + 3/8}$$

to the data. This produces a signal in which the noise can be treated as additive Gaussian with unitary variance. Second, the noise is removed using a conventional denoising algorithm for additive white Gaussian noise. In our case we consider the BLS-GSM algorithm. Third, an inverse transformation is applied to the denoised signal, obtaining the estimate of the signal of interest.

Variance stabilization has often been questioned as a viable method for Poisson noise removal because of the poor numerical results achieved at the low count regime, i.e. for low-intensity signals, which corresponds to the case of low signal-to-noise ratio (SNR). We show that this disappointing performance, reported in many earlier works (e.g., [3]), is not due to the stabilization itself (i.e. to the forward transformation), but rather to the inverse transformation.

The choice of the proper inverse transformation is crucial in order to minimize the bias error which arises when the nonlinear forward transformation is applied. Both the algebraic inverse and the asymptotically unbiased inverse proposed by Anscombe [6] lead to a significant bias at low counts.

In particular, the latter inverse provides unbiased only asymptotically for large counts while at low counts it leads to a larger bias than the former one. We present an extensive experimental analysis using the state of art BLS_GSM denoising algorithm and show that the results can be consistently improved by applying the exact unbiased inverse. In particular, the combination of exact unbiased inverse and BLS-GSM outperforms some of the best existing algorithms specifically targeted at Poisson noise removal, in fluorescence images while maintaining low computational complexity.

The rest of the paper is organized as follows: Section II introduces some essentials (Theory) about Poisson noise, variance stabilization, Gaussian denoising and the conventional inverses of the Anscombe transformation. In Section III we consider optimal inverse transformations: first we propose the exact unbiased inverse. Section IV consists of various experiments, followed by discussion and conclusions in Section V.

Theory

A. Poisson noise

Let $z_i, i = 1, \dots, N$, be the observed pixel values obtained through an image acquisition device. We consider each z_i to be an independent random Poisson variable whose mean $y_i \geq 0$ is the underlying intensity value to be estimated. Explicitly, the discrete Poisson probability of each z_i

$$E\{z_i|y_i\} = \frac{y_i^{z_i} e^{-y_i}}{z_i!} \quad (1)$$

In addition to being the mean of the Poisson variable z_i , the parameter y_i is also its variance:

$$E\{z_i|y_i\} = y_i = var\{z_i|y_i\} \quad (2)$$

Poisson noise can be formally defined as

$$\eta_i = z_i - E\{z_i|y_i\} \quad (3)$$

Thus, we trivially have $E\{\eta_i|y_i\} = 0$ and

$$var\{\eta_i|y_i\} = var\{z_i|y_i\} = y_i.$$

Since the noise variance depends on the true intensity value, Poisson noise is signal dependent. More specifically, the standard deviation of the noise η_i equals $\sqrt{y_i}$.

Due to this, the effect of Poisson noise increases (i.e. the signal-to-noise ratio decreases) as the intensity value decreases

Variance stabilization and the Anscombe transformation

The rationale behind applying a variance-stabilizing transformation is to remove the data-dependence of the noise variance, so that it becomes constant throughout the

whole data $z_i, i=1 \dots N$. Moreover, if the transformation is also normalizing (i.e. it results in a Gaussian noise distribution), we can estimate the intensity values y_i with a conventional denoising method designed for additive white Gaussian noise. Neither exact stabilization nor exact normalization is possible therefore, in practice, approximate or asymptotical results are employed.

One of the most popular variance-stabilizing transformations is the Anscombe transformation

$$z_i \rightarrow 2\sqrt{z_i + 3/8}$$

Applying (4) to Poisson distributed data gives a signal whose noise is asymptotically additive standard normal. The denoising of D produces a signal \hat{D} that can be considered as an estimate of $E\{f(z)|y\}$

Denoising-BLS-GSM

The method for removing noise from digital images, is based on a statistical model of the coefficients of an over complete Multiscale oriented basis. Neighborhoods of coefficients at adjacent positions and scales are modeled as the product of two independent random variables: a Gaussian vector and a hidden positive scalar multiplier. The latter modulates the local variance of the coefficients in the neighborhood, and is thus able to account for the empirically observed correlation between the coefficients amplitudes. Under this model, the Bayesian least squares estimate of each coefficient reduces to a weighted average of the local linear estimates over all possible values of the hidden multiplier variable. We demonstrate through simulations with images contaminated by additive white Gaussian noise that the performance of this method substantially surpasses that of previously published methods, both visually and in terms of mean squared error.

Our procedure for image denoising uses the same top-level structure

- 1) Decompose the image into pyramid sub bands at different scales and orientations;
- 2) Denoise each sub band, except for the low pass residual band;
- 3) Invert the pyramid transform, obtaining the denoised image. We assume the image is corrupted by independent additive white Gaussian noise of known variance.

A vector corresponding to a neighborhood of observed coefficients of the pyramid representation can be expressed as

$$y = x + w = \sqrt{z}u + w \quad (5)$$

Note that the assumed GSM structure of the coefficients, coupled with the assumption of independent additive Gaussian noise, means that the three random variables on the right side of (5) are independent.

Both u and w are zero-mean Gaussian vectors, with associated covariance matrices C_u and C_w . The density of the observed neighborhood vector conditioned on z is a zero-mean Gaussian, with covariance $c(y|z) = zC_u + C_w$

$$p(y|z) = \exp\left(\frac{-y^T(zC_u + C_w)^{-1}y}{2(zC_u + C_w)}\right) \quad (6)$$

The neighborhood noise covariance C_w , is obtained by decomposing a delta function

$$\sigma \sqrt{N_y N_x} \delta(n, m)$$

pyramid sub bands, where (N_y, N_x) are the image dimensions. This signal has the same power spectrum as the noise, but it is free from random fluctuations. Elements of C_w may then be computed directly as sample covariances (i.e., by averaging the products of pairs of coefficients over all the neighborhoods of the sub band).

This procedure is easily generalized for nonwhite noise, by replacing the delta function with the inverse Fourier transform of the square root of the noise power spectral density. Given C_w , the signal covariance can be computed from the observation covariance matrix C_y . We compute from $C(y|z)$ by expectations over z :

$$C(y) = E\{z\}C_u + C_w$$

Without loss of generality, we set $E\{z\}=1$, resulting in:

$$C_u = C_y - C_w \tag{7}$$

We force C_u to be positive semidefinite by performing eigenvector decomposition and setting any possible negative Eigen values (nonexistent or negligible, in most cases) to zero.

i). Bayes Least Squares Estimator

For each neighborhood, we wish to estimate x_c , the reference coefficient at the center of the neighborhood, from, the set of observed (noisy) coefficients. The Bayes least squares (BLS) estimate is just the conditional mean

$$\begin{aligned} E\{x_c|y\} &= \int x_c p(x_c|y) dx_c \\ &= \int \int_0^\infty x_c p(x_c, z|y) dz dx_c \\ &= \int \int_0^\infty x_c p(x_c|y, z) p(z|y) dz dx_c \\ &= \int_0^\infty p(z|y) E\{x_c|y, z\} dz \tag{8} \end{aligned}$$

where we have assumed uniform convergence in order to exchange the order of integration. Thus, the solution is the averages of the Bayes least squares estimate of x when conditioned on z , weighted by the posterior density, $p(z|y)$. We now describe each of these individual components.

Local Wiener Estimate

The key advantage of the GSM model is that the coefficient neighborhood vector x is Gaussian when conditioned on z . This fact, coupled with the assumption of additive Gaussian noise means that the expected value inside the integral of (8) is simply a local linear (Wiener) estimate. Writing this for the full neighborhood vector

$$E\{x|y, z\} = zC_u(zC_u + C_w)^{-1} y \tag{9}$$

Solving we get

$$E\{x_c|y, z\} = \sum_{n=1}^N \frac{z m_{cn} \lambda_n v_n}{z \lambda_n + 1} \tag{10}$$

iii. Posterior Distribution of the Multiplier

The other component of the solution given in (8) is the distribution of the multiplier, conditioned on the observed neighborhood values. We use Bayes' rule to compute this

$$p(z|y) = \frac{p(y|z)p_z(z)}{\int_0^\infty p(y|\alpha)p_z(\alpha)d\alpha} \tag{11}$$

Summarizing our denoising algorithm

- 1) Decompose the image into sub bands.
- 2) For each sub band (except the low pass residual):
 - a) Compute neighborhood noise covariance, C_w , from the image-domain noise covariance.
 - b) Estimate noisy neighborhood covariance, C_y
 - c) Estimate C_u from C_w and C_y using.
 - d) Compute \wedge and M
 - e) For each neighborhood:
 - i) For each value z in the integration range:
 - A) Compute $E\{x_c|y, z\}$ using (10).
 - B) Compute $p(y|z)$
 - ii) Compute $p(z|y)$ using (11)

iii) Compute numerically using (8).

3) Reconstruct the denoised image from the processed sub bands and the low pass residual to get D .

Inverse Transformation

We need to apply an inverse transformation to D in order to obtain the desired estimate of y . The direct algebraic inverse of (4) is

$$Ia(D) = f^{-1}(D) = \left(\frac{D}{2}\right)^2 - \frac{3}{8} \tag{12}$$

but the resulting estimate of y is biased, because the nonlinearity of the transformation f means we generally have

$$E\{f(z)|y\} \neq f(E\{z|y\}). \tag{13}$$

and, thus,

$$f^{-1}(E\{f(z)|y\}) \neq E\{z|y\} \tag{14}$$

Another possibility is to use the adjusted inverse

$$Ib(D) = \left(\frac{D}{2}\right)^2 - \frac{1}{8} \tag{15}$$

which provides asymptotical un-biasedness for large counts. This is the inverse typically used in applications.

III. Optimal Inverse Transformations

While the asymptotically unbiased inverse (15) provides good results for high-count data, applying it to low-count data leads to a biased estimate.

A. Exact unbiased inverse

Provided a successful denoising, i.e. D is treated as $E\{f(z)|y\}$, the exact unbiased inverse of the Anscombe transformation f is an inverse transformation that maps the values $E\{f(z)|y\}$ to the desired values $E\{z|y\}$:

$$Ic: E\{f(z)|y\} \rightarrow E\{z|y\} \tag{16}$$

Since $E\{z|y\}=y$ for any given y , the problem of finding the inverse reduces to computing the values $E\{f(z)|y\}$, which is done by numerical evaluation of the integral corresponding to the expectation operator E :

$$E\{f(z)|y\} = \int_{-\infty}^{\infty} f(z)p(z|y) dz \tag{17}$$

where $p(z|y)$ is the generalized probability density function of z conditioned on y . In our case we have discrete Poisson probabilities $p(z|y)$ so we can replace the integral by summation:

$$E\{f(z)|y\} = \sum_{z=0}^{\infty} f(z)p(z|y) \tag{18}$$

Further, since here $f(z)$ is the forward Anscombe transformation we can write (18) as

$$E\{f(z)|y\} = 2 \sum_{z=0}^{\infty} \left(\sqrt{z + \frac{3}{8}} \cdot \frac{y^z e^{-y}}{z!} \right) \tag{19}$$

Let us remark that if the exact unbiased inverse (16) is applied to the denoised data D with some errors (in the sense that $D \neq E\{f(z)|y\}$, then the estimation error $y = Ic(D)$ can include variance as well as bias components. In general, the unbiasedness of Ic holds only provided that $D = E\{f(z)|y\}$ exactly, as it is assumed.

Experiments

All of our experiments consist of the same three-step denoising procedure: First we apply the forward Anscombe transformation (4) to a noisy image. Then we denoise the transformed image (assuming additive white Gaussian noise of unit variance) with BLSGSM [8],

and finally we apply an inverse transformation in order to get the final estimate. To implement the exact unbiased inverse I_c in practice, it is sufficient to compute (19) for a limited set of values y ; for arbitrary values of y we then use linear interpolation based on these computed values of (19), and for large values of y we approximate I_c by I_b . We evaluate the performance by peak signal-to-noise ratio (PSNR). The PSNR is calculated using the formula

$$10 \log_{10} \left(\frac{\max(y_i)^2}{\sum_i ((\hat{y}_i - y_i)^2 | N)} \right)$$

where N is the total number of pixels in the image.

In our experiments we use the test images shown in Figure 1a, 1b and 1c and evaluate the performance in terms of PSNR. We use the BLS-GSM for the denoising, and the inversion is done with either the exact unbiased inverse or the asymptotically unbiased inverse.

The denoising performance is evaluated in terms of PSNR. Table 1 presents the obtained results. Table shows the increment of PSNR (ISNR) values from the noisy image to the denoised image.

The Four Test Images Used In The Experiments

Figure 1 (a) Lung tissue of an adult female grey fox

Figure 1 (b) Image of Phalloidin staining

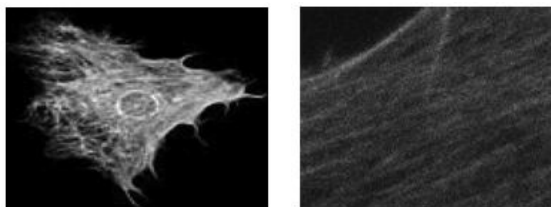
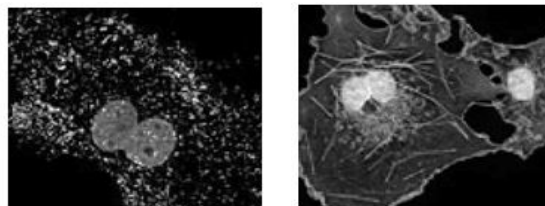


Figure 1 (c) Embryonic Albino Swiss mouse fibroblast Cells.

Figure 1 (b) Image of Phalloidin staining



Summary

All experiments produce consistent results, showing that at low intensities we obtain significantly better results by applying the exact unbiased inverse instead of the asymptotically unbiased inverse, whereas at high intensities there is expectedly no significant improvement. The results also show that combined with a state-of-the-art

Gaussian denoising algorithm, the exact unbiased inverse is competitive with some of the best algorithms targeted at Poisson noise removal. Hence this denoising strategy i.e. with the exact unbiased estimate is very effective for fluorescence images which are basically of low intensities.

Table 1 :

IMAGES σ	FIGURE 1(a)		FIGURE 1(b)		FIGURE 1(c)		FIGURE 1(d)	
	Isnr With Asymptotic Inverse	Isnr With Exact Unbiased Inverse	Isnr With Asymptotic Inverse	Isnr With Exact Unbiased Inverse	Isnr With Asymptotic Inverse	Isnr With Exact Unbiased Inverse	Isnr With Asymptotic Inverse	Isnr With Exact Unbiased Inverse
1	18.3733	18.3788	37.928	37.928	20.8926	20.9045	21.0092	21.0103
2	12.3533	12.3547	37.7762	37.7762	10.0408	10.0415	13.8841	13.8842
5	8.7174	8.718	37.4882	37.4882	2.1305	2.1306	8.4743	8.4743
10	6.3147	6.315	37.2215	37.2215	0.86797	0.86805	6.332	6.332
15	4.8577	4.8579	37.011	37.011	-0.01025	-0.010188	5.2478	5.2478
20	3.3614	3.3615	36.8504	36.8504	-1.052	-1.052	4.4453	4.4453
25	1.9348	1.9349	36.6522	36.6522	-2.1395	-2.1395	3.5624	3.5624

REFERENCES

Luisier, F., C. Vonesch, T. Blu, and M. Unser, .Fast interscale wavelet denoising of Poisson-corrupted images., Signal Processing, vol. 90, no. 2, pp. 415.427, Feb. 2010. | Fryzlewicz, P., and G.P. Nason, .A Haar-Fisz Algorithm for Poisson Intensity Estimation., Journal of Computational and Graphical Statistics, vol. 13, no. 3, pp. 621.638, 2004. | Kolarczyk, E.D., and D.D. Dixon, .Nonparametric estimation of intensity maps using Haar wavelets and Poisson noise characteristics, The Astrophysical Journal, vol. 534, no. 1, pp. 490.505, 2000. | Willett, R.M., and R.D. Nowak, .Platelets: A Multiscale Approach for Recovering Edges and Surfaces in Photon-Limited Medical Imaging., IEEE Trans. Med. Imag., vol. 22, no. 3, pp. 332.350, March 2003. | Willett, R.M., .Multiscale Analysis of Photon-Limited Astronomical Images., Statistical Challenges in Modern Astronomy (SCMA) IV, 2006. | Anscombe, F.J., .The transformation of Poisson, binomial and negative binomial data., Biometrika, vol. 35, no. 3/4, pp. 246.254, Dec. 1948. | Anscombe, F.J., .The transformation of Poisson, binomial and negative binomial data., Biometrika, vol. 35, no. 3/4, pp. 246.254, Dec. 1948. | Portilla, J., V. Strela, M.J. Wainwright, and E.P. Simoncelli, .Image denoising using scale mixtures of Gaussians in the wavelet domain., IEEE Trans. Image Process., vol. 12, no. 11, pp. 1338.1351, Nov. 2003. | Lefkimiatis, S., P. Maragos, and G. Papandreou, .Bayesian inference on multiscale models for Poisson intensity estimation: Applications to photon-limited image denoising., IEEE Trans. Image Process., vol. 18, no. 8, pp. 1724.1741, Aug. 2009